

Triangular $\sqrt{3}$ -Subdivision Schemes: The Regular Case

Qingtang Jiang

Department of Mathematics & Computer Science
University of Missouri–St. Louis
St. Louis, MO 63121
e-mail: jiang@math.umsl.edu

Peter Oswald

Bell Laboratories, Lucent Technologies
600 Mountain Avenue
Murray Hill, NJ 07974
e-mail: poswald@research.bell-labs.com

Abstract

The paper deals with the investigation of triangular $\sqrt{3}$ -subdivision schemes in the stationary shift-invariant setting. In Section 2 we collect the available theory on refinable functions (subdivision surfaces), with emphasis on their Sobolev and Hölder smoothness. Families of interpolatory and approximating $\sqrt{3}$ -subdivision schemes are investigated in Section 3. Some dual $\sqrt{3}$ -subdivision schemes which are related to vector-valued refinable functions are also analyzed. For this purpose, we have developed Matlab routines for numerically investigating properties of vector subdivision schemes.

Keywords: Surface subdivision, $\sqrt{3}$ -refinement, refinable vectors, sum rules, Sobolev- and Hölder regularity.

Classification: 65D17, 42C15, 41A63, 68U05

1 Introduction

This paper is motivated by the recent interest in triangular primal-dual and $\sqrt{3}$ -subdivision schemes for creating smooth parametric surfaces $z = f(x)$. Roughly speaking, given values z_P at the vertices P of a triangulation \mathcal{T}_0 , in a *primal-dual scheme* values z_{P_Δ} are created at the barycenters P_Δ of the triangles Δ , i.e., the dual vertices of \mathcal{T}_0 . Connecting dual vertices with the neighboring original and dual vertices induces a new

triangulation \mathcal{T}_1 . Although \mathcal{T}_1 is not a refinement of \mathcal{T}_0 , we call it $\sqrt{3}$ -refinement of \mathcal{T}_0 , since two steps of the above procedure correspond to triadic refinement of the original triangulation, compare Figure 1. *Primal $\sqrt{3}$ -subdivision schemes* consist of one step of

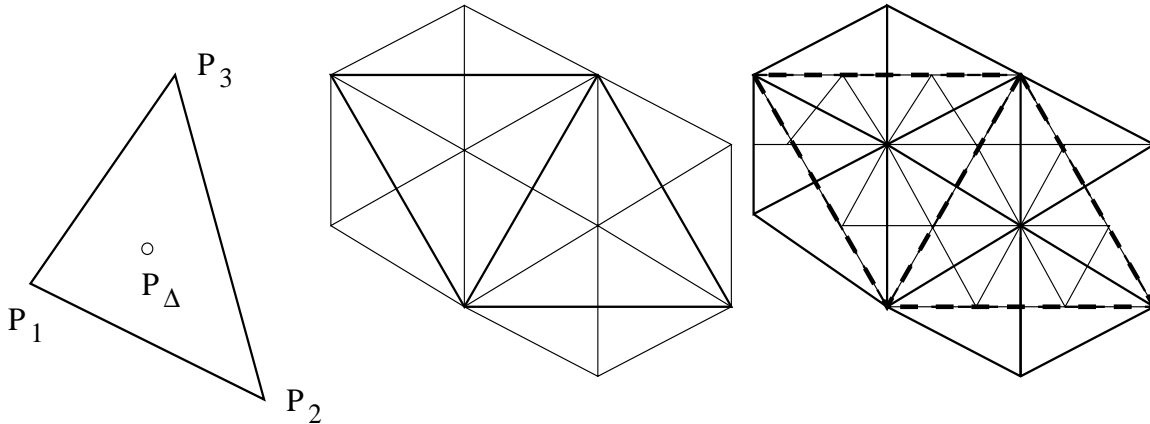


Figure 1: Two steps of $\sqrt{3}$ -refinement

a primal-dual scheme followed by relaxing the values at the old vertices. Schemes where the relaxation step is omitted are called *interpolatory* since z -values at the old vertices are preserved. The simplest candidate of such an interpolatory scheme is given by

$$z_{P_\Delta} = \frac{1}{3} \sum_{P \in \Delta} z_P, \quad (1)$$

which corresponds to linear interpolation. A smoothness analysis of the resulting surfaces beyond stating their obvious continuity has not been done. A more involved interpolatory scheme was introduced by Labsik and Greiner [17]. They claim C^1 -continuity of the resulting surfaces.

Non-interpolatory schemes are called *approximating*. Kobbelt [16] has come up with an approximating $\sqrt{3}$ -subdivision scheme in which the interpolatory rule (1) for dual vertices is followed by a 1-ring update for the old vertices. As a result of his analysis he proves C^2 -continuity of the scheme at regular vertices. All these schemes do not lead to piecewise polynomial surfaces which makes the analysis for $\sqrt{3}$ -subdivision more subtle. It is possible to construct C^3 -smooth quartic spline surfaces compatible with $\sqrt{3}$ -refinement in the shift-invariant setting, however, the associated box spline violates the stability condition.

One can also view the above schemes from another angle: they represent subdivision schemes for vertex values where intermediately values at the triangles or *faces* of the triangulation are computed. Clearly, one could reverse the roles of vertices and faces, and ask for properties of subdivision schemes associated with faces (and edges for that matter). These are called *dual schemes*. In the case of *dyadic* or *2-refinement* where each triangle is refined by quadrisection, this leads to the theory of half-box or triangular box splines, see [22] for an overview. Unfortunately, half-box spline theory has no direct

counterpart for $\sqrt{3}$ -subdivision. The systematic construction of vertex- and face-based schemes from simple components for $\sqrt{3}$ -refinement of triangulations has recently been undertaken in [21], and has brought up new questions concerning the smoothness and other properties of the limit surfaces.

In this paper, we will examine the tools necessary for determining the smoothness and other associated properties of $\sqrt{3}$ -subdivision surfaces on regular, shift-invariant triangulations of \mathbb{R}^2 , where all vertices have valence 6, and apply them to a number of the above mentioned and new examples in a systematic way. It is common practice to separate this issue from the other important step in investigating subdivision schemes, the treatment of *irregular vertices* and boundaries (see, e.g., [23, 32, 28]). Only schemes that work well in the shift-invariant setting are of interest. Thus, we will concentrate on stationary subdivision schemes on shift-invariant triangulations in \mathbb{R}^2 , with a topologic refinement described by the dilation matrix

$$M = \begin{pmatrix} 1 & 2 \\ -2 & -1 \end{pmatrix}. \quad (2)$$

Figure 2 shows a section of this triangulation, together with its refined and coarsened

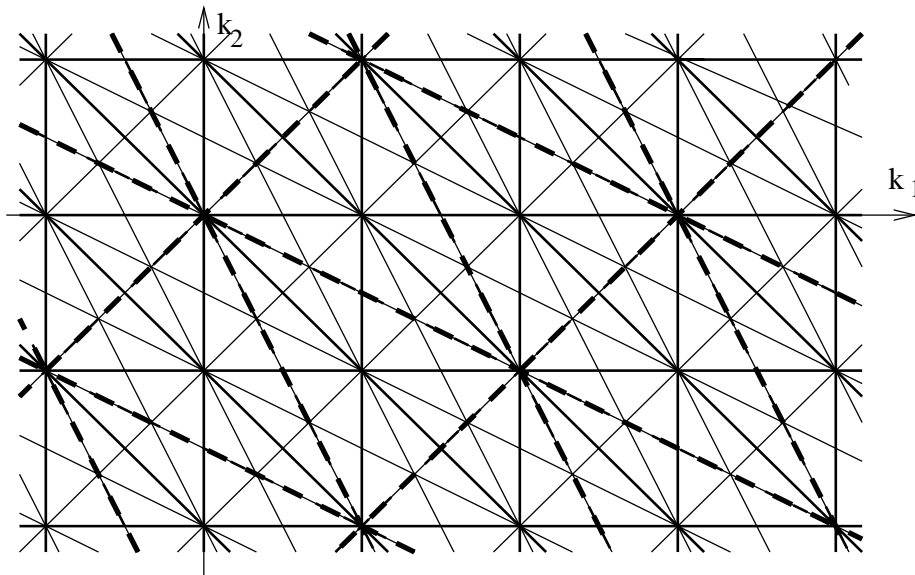


Figure 2: Type-II triangulation (with coarser and finer triangulation)

counterparts, i.e., its images under M^{-1} and M . Note that this M satisfies $\det M = 3 > 0$, i.e., it preserves orientation, and $M^2 = -3 \cdot \text{Id}$ which reveals the connection with triadic refinement. Note that there is an alternative choice for M describing the same $\sqrt{3}$ -refinement with $\det M = -3$ and $M^2 = 3 \cdot \text{Id}$. Since the subsequent analysis remains the same, we will work with (2).

In order to investigate the smoothness of subdivision surfaces, we have to access the smoothness of solutions of the associated refinement equation. In the most general case,

we are lead to vector refinement equations of the form

$$\Phi(x) = \sum_{k \in \mathbb{Z}^d} P_\alpha \Phi(Mx - \alpha), \quad x \in \mathbb{R}^d, \quad (3)$$

where $P := \{P_\alpha : \alpha \in \mathbb{Z}^d\}$, the so-called *mask of the refinement equation*, is a finitely supported sequence of real-valued $r \times r$ coefficient matrices the entries of which depend on the particular subdivision rules, the dilation matrix M is given by the underlying refinement type,

$$\Phi(x) \equiv (\phi_1(x), \dots, \phi_r(x))^T$$

is an $r \times 1$ vector of functions (distributions) on \mathbb{R}^d , and d is the spatial dimension. In the applications to $\sqrt{3}$ -subdivision in Section 3, we have $d = 2$, M is given by (2), and $r \leq 2$.

The investigation of refinement equations and subdivision has been pursued over the last 15 years, with the main focus on dyadic dilation, where $M = 2 \cdot \text{Id}$. More recently, progress on general isotropic integer dilation matrices and the determination of the Sobolev and Hölder smoothness of refinable functions in the vector case ($r > 1$) has been made. Section 2 handily collects the available information on solutions of (3), with special emphasis on the dilation matrix M from (2), and the connection to the smoothness of $\sqrt{3}$ -subdivision surfaces. This material enables us to estimate Sobolev and Hölder smoothness on a fine scale from the coefficient masks for $\sqrt{3}$ -subdivision schemes. In contrast, in the above-mentioned papers [16, 17], the authors are restricted to the case of integer C^k -smoothness and, by combining two $\sqrt{3}$ -subdivision steps, use triadic subdivision as an auxiliary tool, at the expense of considering larger masks. The investigation of Sobolev smoothness, although of less importance for judging the smoothness of subdivision surfaces, has been included since it naturally comes up if one intends to use the resulting refinable functions (and associated wavelets) in Galerkin methods for variational problems.

In Section 3.1 we examine some interpolatory $\sqrt{3}$ -subdivision schemes. In particular, for linear interpolation (1) we found that the Sobolev smoothness of the limiting surfaces is $s_2 = 1.6571\dots$, which should be compared with the value 1.5 for the corresponding linear box spline scheme in the 2-refinement case. Since $H^s(\mathbb{R}^2) \subset C^{s'}(\mathbb{R}^2)$ for any $0 \leq s' < s - 1$, the limiting surfaces are at least $C^{0.6571}$ -smooth. A more subtle analysis shows that the critical smoothness exponent in the Hölder scale is $s_\infty = 0.7381\dots$ which is less than the corresponding value of 1 for the linear box spline. The rotation of the triangulations for $\sqrt{3}$ -refinement seems to smear out the edge singularities of the linear box spline but, at the same time, leads to a more distinctive point singularity at the origin which explains the larger gap between Sobolev and Hölder smoothness exponents.

We re-examined the interpolatory $\sqrt{3}$ -subdivision rule from [17] for which we found Sobolev smoothness $s_2 = 2.5299\dots$. This gives at least $C^{1.5299}$ -smoothness of the subdivision surfaces away from irregular vertices, and complements the C^1 -result claimed in [17]. Based on our numerical evidence, the exact value of the Hölder smoothness exponent of this scheme is $s_\infty = 1.5594\dots$. We also found a new interpolatory scheme which is a bit less expensive, only leads to Sobolev smoothness $s_2 = 1.8959\dots$, but still

promises to yield C^1 -surfaces. Numerically, we obtained $s_\infty = 1.5401\dots$ which is very close to the corresponding value for the scheme from [17].

Some approximating schemes are considered in Section 3.2. For Kobbelt's scheme [16], we found $s_2 = 2.9360\dots$ for the Sobolev smoothness, and $s_\infty = 2.6309\dots$ for the Hölder exponent. We also found a slight generalization of Kobbelt's rule which, at little extra expense, leads to C^3 -surfaces and possesses Sobolev smoothness $s_2 = 3.9518\dots$ and Hölder smoothness $s_\infty = 3.3143\dots$. With respect to smoothness, this is slightly worse than the smoothness properties of the lowest-degree box spline associated with $\sqrt{3}$ -refinement, which happens to have the exactly same stencil formats but, on the downside, features linear dependencies among its shifts.

Finally, in Section 3.3 we give results for dual schemes which are related to vector refinement equations where $r = 2$. We first investigate some low-order composite schemes from [21]. What concerns the smoothness issue, here we benefit from the fact that for composite schemes of the type considered it reduces to studying the smoothness of refinable functions for a related scalar refinement equation. The results support the practical observation [21] that iterated application of very simple, local rules to build a composite scheme leads to highly smooth surfaces very quickly. We also investigate another simple family of face-based schemes which cannot be associated, in any straightforward way, with a scalar refinement equation.

In summary, what we hope to convey with this paper is that tools from the theory of refinable functions are available to support more demanding investigations and design problems for multivariate subdivision schemes. We illustrate this point on the example of the recently introduced $\sqrt{3}$ -subdivision schemes. However, the Matlab functions developed for the computations in this paper are capable of handling other isotropic two-dimensional dilations as well, some of them extend also to arbitrary dimensions. The routines come without warranty and are not yet optimized with respect to user interface, numerical stability, and runtime efficiency, and can be downloaded (together with an extended version of this paper explaining their usage) at

<http://cm.bell-labs.com/who/poswald>

<http://www.math.ums1.edu/~jiang>.

2 Analysis of $\sqrt{3}$ -subdivision

2.1 Notation and basic definitions

Let \mathbb{N} denote the set of positive integers, and \mathbb{Z}_+ the set of non-negative integers. A d -tuple $\mu = (\mu_1, \dots, \mu_d) \in \mathbb{Z}_+^d$ is called a multi-index, the length of μ is $|\mu| := \mu_1 + \dots + \mu_d$. Denote $\mu! := \mu_1! \cdots \mu_d!$, and

$$\binom{\mu}{\nu} := \frac{\mu!}{\nu!(\mu - \nu)!} \text{ if } \nu_j \leq \mu_j.$$

The partial derivative of a differentiable function f with respect to the j th coordinate is denoted by $D_j f$, $j = 1, \dots, d$, and for a multi-index $\mu = (\mu_1, \dots, \mu_d)$, D^μ is the

differential operator $D_1^{\mu_1} \cdots D_d^{\mu_d}$. For a set $\Omega \subset \mathbb{R}^d$, denote

$$[\Omega] := \Omega \cap \mathbb{Z}^d.$$

For $s \geq 0$, we say that a function f is in the Sobolev space $H^s(\mathbb{R}^d)$ if its Fourier transform \widehat{f} satisfies $(1 + |\omega|^2)^{\frac{s}{2}} \widehat{f}(\omega) \in L^2(\mathbb{R}^d)$. Let $s_2(f)$ denote its *critical Sobolev exponent* defined by

$$s_2(f) := \sup\{s : f \in H^s(\mathbb{R}^d)\}.$$

For a vector-valued function $F = (f_1, \dots, f_r)^T$, we analogously denote

$$s_2(F) := \min\{s_2(f_j) : 1 \leq j \leq r\}.$$

The critical Hölder exponent is defined as follows. For a function $f \in C(\mathbb{R}^d)$, we define the j th difference in direction $t \in \mathbb{R}^d$ as

$$\nabla_t^j f := \nabla_t^1(\nabla_t^{j-1} f), \quad \nabla_t^1 f(x) := f(x) - f(x - t), \quad x \in \mathbb{R}^d.$$

The j th modulus of smoothness is given by

$$\omega_j(f, h) := \sup_{|t| \leq h} \|\nabla_t^j f\|_C, \quad h \geq 0.$$

For $s > 0$, we use $\text{Lip}(s)$ to denote the generalized Lipschitz-Hölder class consisting of all bounded functions $f \in C(\mathbb{R}^d)$ with

$$\omega_j(f, h) \leq Ch^s, \quad h > 0,$$

where C is a constant independent of h , and j is any fixed integer greater than s . It is common to set $C^s(\mathbb{R}^d) := \text{Lip}(s)$ for non-integer $s > 0$, and keep the usual definition for spaces of continuously differentiable functions for integer s . The number

$$s_\infty(f) := \sup\{s : f \in \text{Lip}(s)\}$$

is called *critical Hölder exponent of f* . For a vector-valued function $F = (f_1, \dots, f_r)^T$, set

$$s_\infty(F) := \min\{s_\infty(f_j)\}.$$

Analogous definitions hold for L^p -smoothness ($1 \leq p \leq \infty$) but we will not need them here.

The linear space of all sequences and the linear space of all finitely supported sequences on \mathbb{Z}^d are denoted by $\ell(\mathbb{Z}^d)$ and $\ell_0(\mathbb{Z}^d)$, respectively. For $\alpha \in \mathbb{Z}^d$, we denote by δ_α the element in $\ell_0(\mathbb{Z}^d)$ given by $\delta_\alpha(\alpha) = 1$ and $\delta_\alpha(\beta) = 0$ for all $\beta \in \mathbb{Z}^d \setminus \{\alpha\}$. In particular, we write δ for δ_0 .

In order to avoid confusion between scalar, vector, and matrix functions and sequences, we indicate the respective dimensions whenever necessary. E.g., $\ell^p(\mathbb{Z}^d)^{1 \times r}$ is the space of all p -summable $1 \times r$ row vector sequences indexed over \mathbb{Z}^d , $L^p(\mathbb{R}^d)^{r \times 1}$ stands for the space of $r \times 1$ column vector functions whose entries are in $L^p(\mathbb{R}^d)$, and so on. Norms on such product spaces are introduced as usual.

For $F = (f_1, \dots, f_r)^T \in L^p(\mathbb{R}^d)^{r \times 1}$, we say that F is L^p stable provided that there exist positive constants C_1, C_2 such that

$$C_1 \|c\|_{\ell^p(\mathbb{Z}^d)^{1 \times r}} \leq \left\| \sum_{\alpha \in \mathbb{Z}^d} c_\alpha F(\cdot - \alpha) \right\|_{L^p(\mathbb{R}^d)} \leq C_2 \|c\|_{\ell^p(\mathbb{Z}^d)^{1 \times r}}, \quad \forall c \in \ell^p(\mathbb{Z}^d)^{1 \times r}.$$

For $p = 2$, this is equivalent to saying that the set

$$\mathbf{F} = \{f_j(\cdot - \alpha) : \alpha \in \mathbb{Z}^d, j = 1, \dots, r\}$$

forms a Riesz basis in the shift-invariant closed subspace $S(\mathbf{F})$ of $L^2(\mathbb{R}^d)$ spanned by \mathbf{F} . Stability is a central notion in connection with refinable functions, both for the discussion of smoothness issues and for applications to Galerkin methods.

We now start with recalling basic properties of the refinement equation (3). Let M be a fixed $d \times d$ dilation matrix with integer entries and eigenvalues in modulus larger than 1. Denote

$$m := |\det M|.$$

Then the coset spaces $\mathbb{Z}^d/(M\mathbb{Z}^d)$ and $\mathbb{Z}^d/(M^T\mathbb{Z}^d)$ each consist of m elements. Let $\gamma_j + M\mathbb{Z}^d$ and $\eta_j + M^T\mathbb{Z}^d, j = 0, \dots, m-1$, be the m distinct elements of $\mathbb{Z}^d/(M\mathbb{Z}^d)$ and $\mathbb{Z}^d/(M^T\mathbb{Z}^d)$ with $\gamma_0 = 0, \eta_0 = 0$, respectively. For future reference, set $\Gamma := \{\gamma_j, j = 0, 1, \dots, m-1\}$.

Taking the Fourier transform of both sides of (3), we obtain

$$\hat{\Phi}(\omega) = P(M^{-T}\omega) \hat{\Phi}(M^{-T}\omega), \quad \omega \in \mathbb{R}^d, \quad (4)$$

where M^{-T} denotes the transpose of M^{-1} , and

$$P(\omega) := \frac{1}{m} \sum_{\alpha \in \mathbb{Z}^d} P_\alpha e^{-i\alpha\omega}, \quad \omega \in \mathbb{R}^d, \quad (5)$$

is the *symbol* associated with (3). Under our assumptions, $P(\omega)$ is an $r \times r$ matrix function the entries of which are trigonometric polynomials with real coefficients.

In this paper we make the simplifying assumption that $P(0)$ satisfies *Condition E*, i.e., 1 is a simple eigenvalue of $P(0)$ and all other eigenvalues of $P(0)$ lie inside the open unit disk (this definition of Condition E applies similarly to any matrix resp. operator on a finite-dimensional space). Let y^0 be the normalized right (column) eigenvector of $P(0)$ associated with eigenvalue 1 (in short, the *right 1-eigenvector* of $P(0)$). It is well-known that if Condition E holds then there exists a unique compactly supported distribution Φ satisfying the refinement equation (3) normalized so that $\hat{\Phi}(0) = y^0$. This compactly supported distribution is called the *normalized solution* of the refinement equation (3) associated with the mask P .

Without loss of generality, assume that the support of the mask P is in the cube $[0, N]^d$, i.e., $P_\alpha = 0, \alpha \notin [0, N]^d$, for some fixed $N \geq 0$. Denote

$$\Omega_+ := \left\{ \sum_{k=1}^{\infty} M^{-k} x_k : x_k \in [0, N]^d, \forall k \in \mathbb{N} \right\},$$

$$\Omega := \left\{ \sum_{k=1}^{\infty} M^{-k} x_k : x_k \in [-N, N]^d, \forall k \in \mathbb{N} \right\}, \quad (6)$$

and

$$\Omega_1 := \left\{ \sum_{k=1}^{\infty} M^{-k} x_k : x_k \in [-N, N]^d - \Gamma, \forall k \in \mathbb{N} \right\}. \quad (7)$$

It is easy to see that the normalized solution of (3) satisfies $\text{supp } \Phi \subset \Omega_+$.

Let $C_0(\mathbb{T}^d)^{r \times r}$ denote the space of all $r \times r$ matrix functions with trigonometric polynomial entries. For a given refinement equation with symbol $P(\omega) \in C_0(\mathbb{T}^d)^{r \times r}$, the associated *transition operator* T_P is defined on $C_0(\mathbb{T}^d)^{r \times r}$ by

$$T_P X(\omega) := \sum_{j=0}^{m-1} P(M^{-T}(\omega + 2\pi\eta_j)) X(M^{-T}(\omega + 2\pi\eta_j)) P(M^{-T}(\omega + 2\pi\eta_j))^*. \quad (8)$$

Since our masks are assumed to be real-valued, the complex conjugate of the matrix function $P(\omega)$ is given by $P(\omega)^* = P(-\omega)^T$. If H_Ω denotes the subspace of $C_0(\mathbb{T}^d)$ defined by

$$H_\Omega := \left\{ h(\omega) \in C_0(\mathbb{T}^d)^{r \times r} : h(\omega) = \sum_{\alpha \in [\Omega]} h_\alpha e^{-i\alpha\omega} \right\}, \quad (9)$$

then H_Ω is invariant under T_P . Furthermore, the eigenfunctions of T_P corresponding to nonzero eigenvalues lie in H_Ω (see [9], [15]). Thus, to study the eigenvalues and eigenfunctions of T_P , one needs only to consider those for the restriction of T_P to the finite-dimensional space H_Ω . In the following, without causing any confusion, we also use T_P to denote the restricted transition operator.

Let us give some specifics for the matrix M given by (2). For the representers of the cosets, we will choose

$$\gamma_0 = \begin{bmatrix} 0 \\ 0 \end{bmatrix}, \gamma_1 = \begin{bmatrix} 1 \\ 0 \end{bmatrix}, \gamma_2 = \begin{bmatrix} 0 \\ 1 \end{bmatrix}; \quad \eta_0 = \begin{bmatrix} 0 \\ 0 \end{bmatrix}, \eta_1 = \begin{bmatrix} 1 \\ 0 \end{bmatrix}, \eta_2 = \begin{bmatrix} 1 \\ 1 \end{bmatrix}. \quad (10)$$

The transition operator T_P takes the form

$$T_P X(M^T \omega) = \sum_{j=0}^2 P(\omega + \tilde{\omega}^j) X(\omega + \tilde{\omega}^j) P(\omega + \tilde{\omega}^j)^*,$$

where

$$\tilde{\omega}^0 = (0, 0)^T, \quad \tilde{\omega}^1 = \left(\frac{2\pi}{3}, \frac{4\pi}{3}\right)^T, \quad \tilde{\omega}^2 = \left(\frac{4\pi}{3}, \frac{2\pi}{3}\right)^T. \quad (11)$$

Since for M given by (2) we have $M^{-1} = -\frac{1}{3}M$, $M^{-2n} = (-3)^n \cdot \text{Id}$, we find that

$$\Omega = \frac{1}{2}M[-N, N]^2 + \frac{1}{2}[-N, N]^2.$$

See Figure 3 for an illustration of Ω .

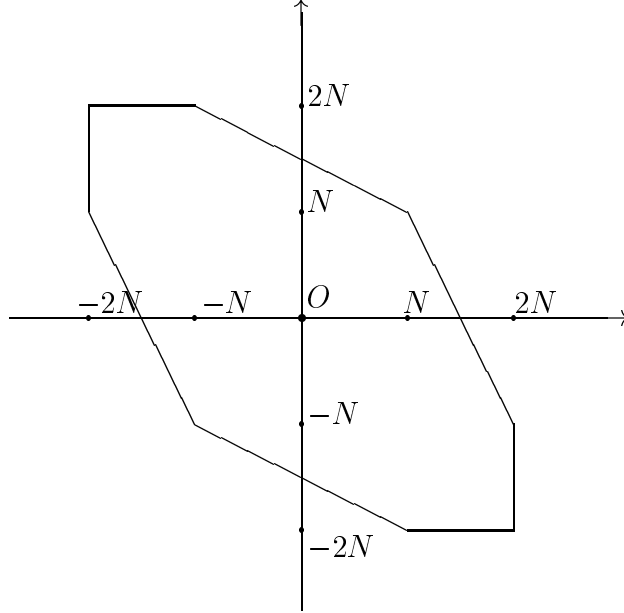


Figure 3: Domain Ω for $\sqrt{3}$ -refinement

For $\gamma \in \Gamma$, let $A_{P,\gamma}$ be operators on $\ell_0(\mathbb{Z}^d)^{r \times 1}$ defined by

$$(A_{P,\gamma}v)_\alpha = \sum_{\beta \in \mathbb{Z}^d} P_{\gamma+M\alpha-\beta} v_\beta, \quad \alpha \in \mathbb{Z}^d, \quad v \in \ell_0(\mathbb{Z}^d)^{r \times 1}. \quad (12)$$

Let V_1 be the subspace of $\ell(\mathbb{Z}^d)^{r \times 1}$ consisting of (v_α) with support in $[\Omega_1]$ and satisfying

$$\sum_{\alpha \in [\Omega_1]} b^0 v_\alpha = 0,$$

where b^0 is the left (row) eigenvector of $P(0)$ associated with eigenvalue 1 (in short, the *left 1-eigenvector* of $P(0)$). If P satisfies sum rules of order 1, i.e.,

$$b^0 P(2\pi M^{-T} \eta_j) = 0, \quad j = 1, \dots, m-1,$$

then V_1 is invariant under the operators $A_{P,\gamma}$, $\gamma \in \Gamma$ (for more on sum rules, see Section 2.2).

For a finite set \mathcal{A} of operators acting on a fixed finite-dimensional space V , the *joint spectral radius* $\rho_\infty(\mathcal{A})$ of \mathcal{A} is defined by

$$\rho_\infty(\mathcal{A}) := \lim_{l \rightarrow \infty} \|\mathcal{A}^l\|_\infty^{1/l},$$

where

$$\|\mathcal{A}^l\|_\infty := \max\{\|A_1 \cdots A_l\| : A_n \in \mathcal{A}, 1 \leq n \leq l\}.$$

Here, the operator norm $\|\cdot\|$ is induced by the norm on V , the value of $\rho_\infty(\mathcal{A})$ does not depend on the choice of the latter. Denote by ρ_1 the joint spectral radius of the family $\{A_{P,\gamma}|_{V_1}, \gamma \in \Gamma\}$.

With the refinement equation (3) we associate the refinement operator Q_P defined on $L^p(\mathbb{R}^d)^{r \times 1}$ by

$$Q_P F := \sum_{\alpha \in \mathbb{Z}^d} P_\alpha F(M \cdot - \alpha). \quad (13)$$

The *cascade algorithm* consists in the repeated application of Q_P , i.e., it produces the sequence $Q_P^n F := Q_P(Q_P^{n-1} F)$, $n = 1, 2, \dots$, from an initial $F \in L^p(\mathbb{R}^d)^{r \times 1}$. If for *some* compactly supported initial $F \in L^p(\mathbb{R}^d)^{r \times 1}$ the cascade algorithm converges in the L^p -norm, then the vector function obtained in the limit is an $L^p(\mathbb{R}^d)^{r \times 1}$ -solution of the refinement equation (3). One can show that the convergence of the sequence $(Q_P^n F)$ in the L^p -norm implies that F satisfies

$$\sum_{\alpha \in \mathbb{Z}^d} b^0 F(\cdot - \alpha) = c_0 \quad (14)$$

for some non-zero constant c_0 , where b^0 is the left 1-eigenvector of $P(0)$. We say that the cascade algorithm associated with P converges in L^p -norm if $(Q_P^n F)$ converges in L^p -norm for *any* compactly supported $F \in L^p(\mathbb{R}^d)^{r \times 1}$ satisfying (14).

The following theorem (see e.g., [27], [13]) is central for the theory of (3).

Theorem 1 *The normalized solution Φ of (3) is L^2 stable if and only if P satisfies sum rules of order at least 1, the transition operator T_P satisfies Condition E and the corresponding 1-eigenfunction, i.e., the matrix function $X^0(\omega) \in H_\Omega$ for which $T_P X^0 = X^0$, is positive (or negative) definite for all $\omega \in \mathbb{T}^d$.*

The cascade algorithm associated with the mask P converges in L^2 -norm (respectively in L^∞ -norm) if and only if P satisfies sum rule of order at least 1 and the transition operator T_P satisfies Condition E (respectively $\rho_1 < 1$, where ρ_1 is the joint spectral radius of the family $\{A_{P,\gamma}|_{V_0}, \gamma \in \Gamma\}$).

From Theorem 1, we see that stability implies the convergence of the cascade algorithm. Knowing about the stability of the normalized solution of (3) also simplifies some of the statements in Section 2.3. It was shown in [12] that if Φ is L^p stable and belongs to $L^q(\mathbb{R}^d)^{r \times 1}$ ($1 \leq q \leq \infty$), then Φ is also L^q stable. Thus to check L^p stability, one needs only to check the L^2 stability, i.e., the conditions in Theorem 1, provided that Φ is in $L^{\max(2,p)}(\mathbb{R}^d)^{r \times 1}$. However, the crucial condition for stability in Theorem 1 is not easy to check.

The cascade algorithm is closely related to the theory of stationary subdivision. The subdivision operator S_P is the linear operator on $\ell_0(\mathbb{Z}^d)^{1 \times r}$ defined by

$$(S_P u)_\alpha := \sum_{\beta \in \mathbb{Z}^d} u_\beta P_{\alpha - M\beta}, \quad \alpha \in \mathbb{Z}^d. \quad (15)$$

The sequence $S_P^n u := S_P(S_P^{n-1} u)$, $n = 1, 2, \dots$, is the result of the subdivision scheme with mask P . Let χ be the characteristic function of $[0, 1)^d$. For $u \in \ell(\mathbb{Z}^d)^{1 \times r}$, denote

$$\chi *' u := \sum_{\alpha} \chi(\cdot - \alpha) u_\alpha.$$

We say the subdivision scheme converges in L^p -norm (uniformly if $p = \infty$) if for *any* $u \in \ell^p(\mathbb{Z}^d)^{1 \times r}$, there exists a vector-valued function $F_u \in L^p(\mathbb{R}^d)^{1 \times r}$ ($F_u \in C(\mathbb{R}^d)^{1 \times r}$ if $p = \infty$) such that

$$\|\chi *' (S_P^n u)(M^n \cdot) - F_u\|_{L^p(\mathbb{R}^d)^{1 \times r}} \rightarrow 0 \quad \text{as } n \rightarrow \infty,$$

and for some $u \in \ell^p(\mathbb{Z}^d)^{r \times 1}$ we have $F_u \neq 0$.

A comprehensive study of stationary subdivision schemes can be found in [3]. The characterization of L^p -norm convergence of vector subdivision schemes in terms of the joint spectral radius is given in [13], [19]. In fact, the characterization is the same as the one for the convergence of the cascade algorithm. In other words, the convergence of subdivision schemes is equivalent to the convergence of the cascade algorithm.

If the subdivision scheme converges, then ϕ_j , the j th component of the normalized solution Φ of (3), is $F_{\delta e^j} y^0$, where y^0 is the normalized right 1-eigenvector of $P(0)$ and e^j is the j th row of the $r \times r$ identity matrix. For $u \in \ell_0(\mathbb{Z}^d)^{1 \times r}$, the limit vector-valued function F_u is a vector of linear combinations of the integer shifts of Φ^T . This explains why results about the smoothness of the solutions of the associated refinement equation directly translate into statements about the smoothness of the limiting surfaces.

2.2 Sum rules

Let Φ be the normalized solution of (3). We say that Φ has *accuracy of order k* provided that for all multi-indices μ with $|\mu| < k$ there exist sequences $c^\mu \in \ell(\mathbb{Z}^d)^{1 \times r}$ such that

$$\frac{x^\mu}{\mu!} = \sum_{\alpha \in \mathbb{Z}^d} c_\alpha^\mu \Phi(x - \alpha), \quad x \in \mathbb{R}^d.$$

The accuracy order of Φ is related to the sum rule order of P . For $r = 1$, we say that P has sum rule of order k provided that

$$P(0) = 1, \quad D^\mu P(2\pi M^{-T} \eta_j) = 0, \quad j = 1, \dots, m-1, \quad |\mu| < k,$$

where η_j are the representers of the coset spaces $\mathbb{Z}^d / (M^T \mathbb{Z}^d)$. For $r > 1$, we say that P has *sum rules of order k* provided there exists a $1 \times r$ vector $B(\omega)$ of trigonometric polynomials such that $B(0) \neq 0$ and

$$D^\mu \left(B(M^T \cdot) P(\cdot) \right) (2\pi M^{-T} \eta_j) = \delta(j) D^\mu B(0), \quad j = 0, \dots, m-1, \quad |\mu| < k. \quad (16)$$

Theorem 2 *Let Φ be the normalized (distributional) solution of (3). If (16) holds for some $k \geq 1$ with a $B(\omega)$ such that $B(0)y^0 = 1$, then Φ has accuracy k . Conversely, if Φ has accuracy k , and if*

$$\text{span}\{\hat{\Phi}(2\pi(M^T)^{-1}\eta_j + 2\pi\beta) : \beta \in \mathbb{Z}^d\} = \mathbb{C}^r \quad \forall 0 \leq j \leq m-1, \quad (17)$$

then (16) holds with a $B(\omega)$ such that $B(0)y^0 = 1$. If $\Phi \in L^2(\mathbb{R}^d)^{r \times 1}$ is L^2 stable then (17) is automatically satisfied.

We have quoted these facts because condition (16) is needed to correctly determine the smoothness of refinable functions, compare Section 2.3. We will not go into discussing the approximation power of the spaces $S(\Phi)$ generated by the sets Φ resp. of subdivision schemes where the above notations originally came up (see e.g., [15] and the references therein for the details).

Let us mention the simplifications if M is *isotropic*, i.e., M is similar to a diagonal matrix $\text{diag}(\sigma_1, \dots, \sigma_s)$ with $|\sigma_1| = \dots = |\sigma_d| = m^{1/d}$. Then there exists an invertible matrix $\Lambda = (\lambda_{jl})_{1 \leq j, l \leq d}$ such that

$$\Lambda M \Lambda^{-1} = \text{diag}(\sigma_1, \dots, \sigma_d). \quad (18)$$

For $j = 1, \dots, d$, let $D_{\Lambda, j}$ be the linear differential operator given by $D_{\Lambda, j} := \sum_{l=1}^d \lambda_{jl} D_l$. For a multi-index μ , define $D_{\Lambda}^{\mu} := D_{\Lambda, 1}^{\mu_1} \dots D_{\Lambda, d}^{\mu_d}$, and $\sigma^{\mu} := \sigma_1^{\mu_1} \dots \sigma_d^{\mu_d}$. Then (16) is equivalent to that there exist $1 \times r$ complex vectors b^{ν} , $|\nu| < k$ with $b^0 \neq 0$, such that (see [15])

$$\sum_{0 \leq \nu \leq \mu} \binom{\mu}{\nu} (i\sigma)^{-\nu} b^{\mu-\nu} D_{\Lambda}^{\nu} P(2\pi M^{-T} \eta_j) = \delta(j) \sigma^{-\mu} b^{\mu}, \quad |\mu| < k, 0 \leq j \leq m-1. \quad (19)$$

For the matrix given by (2), we can choose

$$\Lambda := \frac{1}{2} \begin{pmatrix} 2 & 1 - \sqrt{3}i \\ 2 & 1 + \sqrt{3}i \end{pmatrix} = \begin{pmatrix} 1 & -\tilde{z} \\ 1 & -\tilde{z}^2 \end{pmatrix}, \quad \tilde{z} := e^{i2\pi/3},$$

with $\sigma_1 = \sqrt{3}i$, $\sigma_2 = -\sqrt{3}i$. In this case (19) turns into

$$\sum_{0 \leq \nu \leq \mu} \binom{\mu}{\nu} (-1)^{\mu_1 - \nu_1} \sqrt{3}^{|\mu| - |\nu|} b^{\mu-\nu} (D_1 - \tilde{z} D_2)^{\nu_1} (D_1 - \tilde{z}^2 D_2)^{\nu_2} P(\tilde{\omega}^j) = \delta(j) i^{|\mu|} b^{\mu}, \quad (20)$$

where $|\mu| < k$, $j = 0, 1, 2$, and $\tilde{\omega}^j$ is defined by (11). The system of linear equations (20) can be further simplified in some special cases, see Section 3. For further reference, let us mention that, given any complex trigonometric polynomial

$$v(\omega) = \sum_{\alpha \in \mathbf{Z}^2} v_{\alpha} e^{-i\alpha\omega},$$

its values $v(\tilde{\omega}^j)$, $j = 0, 1, 2$, can conveniently be evaluated from its coefficients by using

$$\begin{aligned} v(\tilde{\omega}^j) &= \sum_{\alpha \in \mathbf{Z}^2} v_{\alpha} e^{-i2\pi/3 \cdot (\alpha_1 + 2\alpha_2)j} = \sum_{\alpha \in \mathbf{Z}^2} v_{\alpha} \tilde{z}^{-(\alpha_1 + 2\alpha_2)j} \\ &= \left(\sum_{\alpha_2 - \alpha_1 = 0 \pmod{3}} v_{\alpha} \right) + \tilde{z}^j \left(\sum_{\alpha_2 - \alpha_1 = 1 \pmod{3}} v_{\alpha} \right) + \tilde{z}^{2j} \left(\sum_{\alpha_2 - \alpha_1 = 2 \pmod{3}} v_{\alpha} \right). \end{aligned}$$

2.3 Criteria for Sobolev and Hölder smoothness

Assume that the mask P is supported in $[0, N]^d$ and satisfies (16) with a vector $B(\omega)$ of trigonometric polynomials for some $k \in \mathbb{N}$. Let T_P be the transition operator defined above, and H_Ω be the invariant subspace of T_P defined by (9). Let H_Ω^k be the subspace of H_Ω defined by

$$H_\Omega^k := \{h \in H_\Omega : D^\nu(Bh)(0) = D^\nu(hB^*)(0) = 0, D^\mu(BhB^*)(0) = 0, |\nu| < k, |\mu| < 2k\}. \quad (21)$$

Then H_Ω^k is invariant under T_P . The next theorem gives an estimate for the Sobolev exponent $s_2(\Phi)$ for isotropic M .

Theorem 3 *Let $\Phi \in L^2(\mathbb{R}^s)^{r \times 1}$ be the normalized solution of (3) with mask P and an isotropic dilation matrix M . Assume that P satisfies (16) with a vector $B(\omega)$, i.e., P has sum rules of at least order k . Let H_Ω^k be the space defined by (21), and $\rho(T_P|_{H_\Omega^k})$ denote the spectral radius of $T_P|_{H_\Omega^k}$. Then*

$$s_2(\Phi) \geq -\frac{d}{2} \log_m \rho(T_P|_{H_\Omega^k}). \quad (22)$$

If Φ is L^2 stable, then we have equality:

$$s_2(\Phi) = -\frac{d}{2} \log_m \rho(T_P|_{H_\Omega^k}). \quad (23)$$

There is a more explicit description of the spectrum of $T_P|_{H_\Omega^k}$ which may simplify the use of the previous theorem. Suppose that $P(0)$ possesses a complete set of eigenvectors and eigenvalues. Denote the eigenvalues by $\lambda_j, 1 \leq j \leq r$, where $\lambda_1 = 1 > |\lambda_2| \geq \dots \geq |\lambda_r|$. Set

$$S_k := \text{spec}(T_P|_{H_\Omega}) \setminus \bar{S}_k, \quad (24)$$

where

$$\bar{S}_k := \{\sigma^{-\alpha} \bar{\lambda}_j, \overline{\sigma^{-\alpha} \lambda_j}, \sigma^{-\beta}, \quad \alpha, \beta \in \mathbb{Z}_+^d, |\alpha| < k, |\beta| < 2k, 2 \leq j \leq r\}$$

is a set of redundant eigenvalues if P satisfies sum rules of order at least k . Note that, when values are deleted from $\text{spec}(T_P|_{H_\Omega})$ as indicated in (24), their multiplicity is taken into account.

Theorem 4 *Let $\Phi \in L^2(\mathbb{R}^d)^{r \times 1}$ be the normalized solution of (3) with mask P and an isotropic dilation matrix M . Assume that P satisfies (16) with a vector $B(\omega)$ of trigonometric functions for some $k \in \mathbb{N}$. Let S_k be the set defined by (24), and set $\rho_0 = \max\{|\lambda| : \lambda \in S_k\}$. Then*

$$s_2(\Phi) \geq -\frac{d}{2} \log_m \rho_0. \quad (25)$$

If Φ is L^2 stable, then we have equality:

$$s_2(\Phi) = -\frac{d}{2} \log_m \rho_0. \quad (26)$$

For the scalar case ($r = 1$), H_Ω^k is the space

$$H_\Omega^k = \{h \in H_\Omega : D^\mu h(0) = 0, \quad |\mu| < 2k\},$$

and \overline{S}_k is

$$\overline{S}_k = \{\sigma^{-\beta} : |\beta| < 2k\}.$$

Theorem 3 is given in [7], [29] for $r = 1, d = 1$, and in [4], [9] for $r = 1, d \geq 1$. Theorem 4 for $r = 1, d \geq 1$ is contained in [14]. For the vector case, see [10]. These theorems lead to efficient ways of computing highly accurate values for the Sobolev smoothness $s_2(\Phi)$ by standard eigenvalue solvers.

Next we discuss a result about the Hölder smoothness estimate from [10]. Suppose that the mask P satisfies sum rules of order at least $k \geq 1$ with some $B(\omega)$, and $\text{supp } P \subset [0, N]^d$. Recall that Γ is the fixed set of representers for the coset space $\mathbb{Z}^d/M\mathbb{Z}^d$, and Ω_1 is defined by (7). Let V_k be the subspace of $\ell(\mathbb{Z}^d)^{r \times 1}$ consisting of v with support in $[\Omega_1]$ and satisfying

$$D^\nu(B(\omega)v(\omega))|_{\omega=0} = 0, \quad |\nu| < k, \quad (27)$$

where $v(\omega) := \sum_{\alpha \in [\Omega_1]} v_\alpha e^{-i\alpha\omega}$. Then V_k is finite-dimensional and invariant under the operators $A_{P,\gamma}, \gamma \in \Gamma$, defined by (12). Denote by ρ_k the joint spectral radius of the family $\mathcal{A}_k := \{A_{P,\gamma}|_{V_k}, \gamma \in \Gamma\}$.

Theorem 5 *Let $\Phi \in C(\mathbb{R}^d)^{r \times 1}$ be the normalized solution of (3) with mask P and an isotropic dilation matrix M . Suppose P satisfies (16) with a vector of trigonometric polynomials $B(\omega)$ for some $k \in \mathbb{N}$. Then*

$$s_\infty(\Phi) \geq -d \log_m \rho_k. \quad (28)$$

If Φ is L^∞ stable, and

$$-d \log_m \rho_k < k, \quad (29)$$

then equality holds in (28), i.e.,

$$s_\infty(\Phi) = -d \log_m \rho_k. \quad (30)$$

Note that in Theorems 3 and 5, the optimal smoothness exponents are completely characterized under the condition that Φ is stable. For the case that Φ is unstable, see the characterizations in [25], [11]. The practical computations reported in Section 3 of bounds for $s_\infty(\Phi)$ using sequences of lower and upper estimates

$$\begin{aligned} \underline{\rho}_k^l &:= \max\{\rho(A_1 \cdots A_l)^{1/l} : A_n \in \mathcal{A}_k, 1 \leq n \leq l\} \\ &\leq \rho_k \leq \overline{\rho}_k^l := \max\{\|A_1 \cdots A_l\|_2^{1/l} : A_n \in \mathcal{A}_k, 1 \leq n \leq l\}, \end{aligned} \quad (31)$$

for the joint spectral radius ρ_k are much more involved than the computational tools needed for determining $s_2(\Phi)$. Here, $\|\cdot\|_2$ is the spectral norm for matrices. For scalar refinement equations and non-negative symbols $P(\omega)$, significant shortcuts are possible (see [30, 8, 1] and the references cited there). Then the optimal $s_\infty(\Phi)$ (or lower bounds for it if Φ is not stable) can be characterized in terms of the spectral radius of the operators $A_{P,\gamma}|_{V_k}$ themselves. We will further comment on this in connection with the examples of Section 3.

2.4 Computational tools

As we have seen above, the basic properties of subdivision schemes and refinement equations can be reduced to studying the spectral properties of certain finite-dimensional operators. To support this task, and enable the systematic use of the available theory in the evaluation and design of subdivision and wavelet schemes, there have been several attempts to develop specific computational tools. We refer to [26, 1, 31] which cover certain aspects of computing Sobolev and Hölder smoothness exponents.

The computational tools used for this paper have originated from earlier versions developed in connection with [20, 18] and [15, 10]. They represent a collection of Matlab functions and input files which are based on the theoretical material of Section 2.1-2.3, and suitable for $d = 2$ and isotropic dilation matrices M (part of them carries over to arbitrary dimensions $d \leq 3$). The routines allow to determine the sum rule order of a mask P , numerically investigate L_2 -stability, provide numerical evidence for Sobolev and Hölder smoothness exponents, and visualize the components of the associated Φ . We have extensively used them in connection with the material of the next section. For details, we refer to the indicated websites.

3 Examples

3.1 Interpolatory rules

We will investigate several interpolatory rules with small mask support for $\sqrt{3}$ -refinement including the linear interpolation rule (1), the proposal from [17], and a scheme intermediate to both of them. Although there exists a general theory for constructing such schemes in the case of arbitrary dilation, see [5, 6] for references on this subject, it does not cover these particular schemes, and details have not been worked out for (2).

Since we are only interested in schemes which have natural generalizations to arbitrary triangulations and, thus, obey certain symmetries in the shift-invariant setting, the rules for dual vertices schematically depicted in Figure 4 are the simplest meaningful candidates. By requiring sum rules of certain order for the corresponding subdivision scheme we will determine suitable values for the parameters a, b, c . Since the scheme in Figure 4 c) contains the other two upon setting $b = c = 0$ resp. $c = 0$, the analysis can be done for the former. The symbol for the associated scalar refinement relation is given by the coefficient array

$$P(\omega) \hat{=} \frac{1}{3} \begin{bmatrix} 0 & 0 & 0 & 0 & c & c & 0 \\ 0 & 0 & c & b & 0 & b & c \\ 0 & c & 0 & a & a & 0 & c \\ 0 & b & a & \mathbf{1} & a & b & 0 \\ c & 0 & a & a & 0 & c & 0 \\ c & b & 0 & b & c & 0 & 0 \\ 0 & c & c & 0 & 0 & 0 & 0 \end{bmatrix}, \quad (32)$$

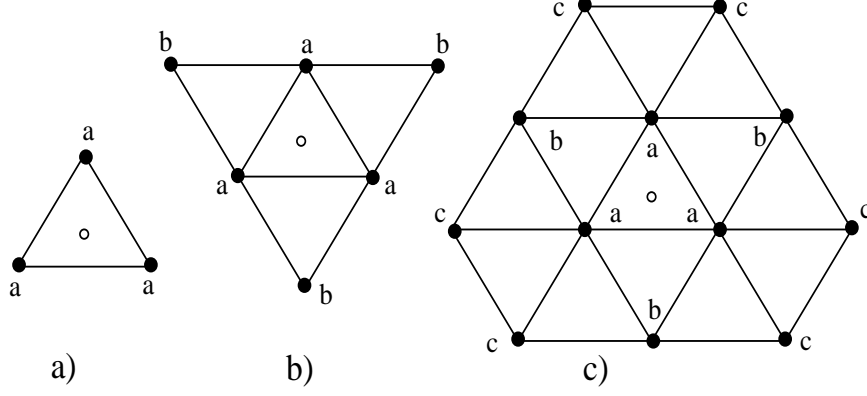


Figure 4: Interpolatory rules: Stencil for updating dual vertices

corresponding to the centered index box $[-3, 3]^2$, i.e., the matrix entry with index $(i_1, i_2) \in [1, 7]^2$ corresponds to the coefficient of $P(\omega)$ with index $(i_1 - 4, i_2 - 4) \in [-3, 3]^2$. Note that for the scalar case and real-valued masks we have $S(\omega) = P(-\omega)$. In the sequel, we always show the coefficient sets of trigonometric polynomials related to some centered index box $[-N, N]^2$, and use bold-faced letters to highlight the coefficient with index $(0, 0)$, without further elaborating on this.

For scalar P , sum rules of order $k > 0$ are satisfied if

$$P(0) = 1, \quad \tilde{D}^\nu P(\tilde{\omega}^j) = 0, \quad j = 1, 2, \quad 0 \leq |\nu| < k, \quad (33)$$

where $\tilde{D}^\nu := i^{|\nu|} D^\nu$. Although the verification of this algebraic condition is straightforward, we show some details. Applied to our example, we compute

$$P(\tilde{\omega}^j) = \frac{1}{3} + (a + b + 2c)(\tilde{z}^j + \tilde{z}^{2j}),$$

and the conditions in (33) are satisfied for $k = 1$ if

$$a + b + 2c = \frac{1}{3}. \quad (34)$$

Incidentally, (34) automatically implies sum rules of order $k = 2$, since $\tilde{D}^\nu P(\tilde{\omega}^j) = 0$ for all $j = 0, 1, 2$, and $|\nu| = 1$. Indeed, one computes

$$\tilde{D}^{(1,0)} P(\omega) \hat{=} \frac{1}{3} \begin{bmatrix} 0 & 0 & 0 & 0 & -3c & -3c & 0 \\ 0 & 0 & -2c & -2b & 0 & -2b & -2c \\ 0 & -c & 0 & -a & -a & 0 & -c \\ 0 & 0 & 0 & \mathbf{0} & 0 & 0 & 0 \\ c & 0 & a & a & 0 & c & 0 \\ 2c & 2b & 0 & 2b & 2c & 0 & 0 \\ 0 & 3c & 3c & 0 & 0 & 0 & 0 \end{bmatrix},$$

analogously for $\nu = (0, 1)$, and using the formulas for evaluating at $\omega = \tilde{\omega}^j$, $j = 0, 1, 2$, the result is immediate.

a	b	c	k_{\max}	$\tilde{\nu}_{stab}(\Phi)$	$s_2(\Phi)$	$s_\infty(\Phi)$
1/3	—	—	2	0.1262	1.6571	0.7381
4/9	-1/9	—	3	0.2647	1.8959	1.5401
32/81	-1/81	-2/81	4	0.2167	2.5299	1.5594

Table 1: Sum rule order, stability indicator, Sobolev and Hölder smoothness for some interpolatory schemes

The case $k = 3$ requires the examination of second derivatives, where we have

$$\begin{aligned}\tilde{D}^{(2,0)}P(\tilde{\omega}^j) &= \tilde{D}^{(0,2)}P(\tilde{\omega}^j) = \frac{2}{3}(a + 4b + 14c)(\tilde{z}^j + \tilde{z}^{2j}), \\ \tilde{D}^{(1,1)}P(\tilde{\omega}^j) &= -\frac{1}{3}(a + 4b + 14c)(\tilde{z}^j + \tilde{z}^{2j}), \quad j = 0, 1, 2.\end{aligned}$$

Thus, P has sum rules of order $k = 3$ if a, b, c satisfy (41) and

$$a + 4b + 14c = 0. \quad (35)$$

Finally, for the 3-th order derivatives we find

$$\begin{aligned}\tilde{D}^{(2,1)}P(\tilde{\omega}^j) &= -\tilde{D}^{(1,2)}P(\tilde{\omega}^j) = \frac{1}{3}(a - 8b + 20c)(\tilde{z}^j - \tilde{z}^{2j}), \\ \tilde{D}^{(3,0)}P(\tilde{\omega}^j) &= \tilde{D}^{(0,3)}P(\tilde{\omega}^j) = 0, \quad j = 0, 1, 2.\end{aligned}$$

which gives another independent condition,

$$a + 20c = 8b. \quad (36)$$

Thus, the maximum order k_{\max} of sum rules for interpolatory schemes with coefficient patterns as shown in Figure 4 a)-c) is achieved for

$$k_{\max} = 2 \quad : \quad a = 1/3 \quad (b = c = 0), \quad (37)$$

$$k_{\max} = 3 \quad : \quad a = 4/9, b = -1/9 \quad (c = 0), \quad (38)$$

$$k_{\max} = 4 \quad : \quad a = 32/81, b = -1/81, c = -2/81, \quad (39)$$

respectively. Clearly, (37) is the rule (1), and (39) reproduces the interpolatory rule introduced in [17].

Table 1 shows values of the smoothness exponents and estimates for the L_2 -stability indicators. The Sobolev smoothness exponent $s_2(\Phi)$ has been computed on the basis of Theorem 4. The value for the critical Hölder exponent $s_\infty(\Phi)$ has been derived from the computations reported in Table 2 (see below), and verified against the results from using the IGPM-Villemoes machine [1]. From these smoothness computations, we know (without assuming stability) that the subdivision schemes are convergent in C in all three cases, and the refinable functions Φ are at least continuous. Since the subdivision

schemes are interpolatory, $\Phi(x)$ is also interpolating, i.e., $\Phi(\alpha) = \delta_\alpha$ for $\alpha \in \mathbb{Z}^2$. Thus, the shifts $\Phi(\cdot - \alpha)$, $\alpha \in \mathbb{Z}^2$, are linearly independent. Altogether, this implies that Φ is stable. The numerical values for the L_2 -stability indicators

$$\tilde{\nu}_{stab}(\Phi) = \min_{\omega \in \mathbb{T}^2} |X_0(\omega)|$$

(see Theorem 1) reported in Table 1 are in good agreement with this theoretical argument. Since stability holds, the last two columns of Table 1 contain the actual smoothness exponents, and not only lower bounds. Figure 5 shows the graphs of the respective refinable functions.

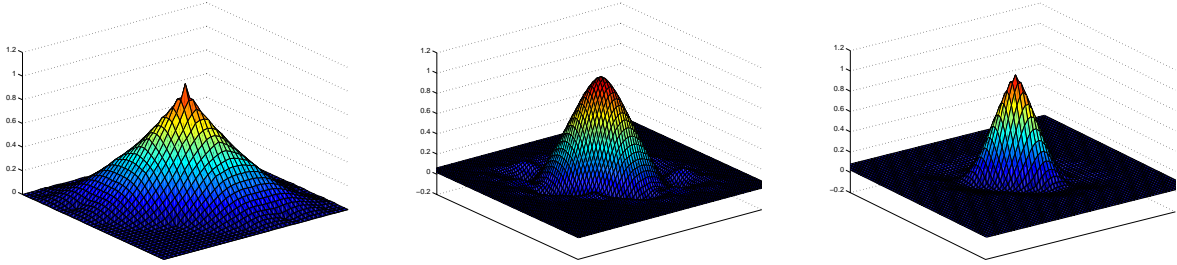


Figure 5: Basis functions for interpolatory schemes.

Let us add a few comments on the numerical computations for the Hölder exponent which is characterized by the joint spectral radius formula in Theorem 5. In Table 2 we show the numbers

$$\bar{s}_\infty^l(\Phi) := -d \log_m \bar{\rho}_k^l \leq s_\infty(\Phi) \leq \underline{s}_\infty^l(\Phi) := \underline{\rho}_k^l$$

for $l = 1, \dots, 13$ and all three interpolatory schemes. The numbers $\bar{\rho}_k^l, \underline{\rho}_k^l$ are defined in (31), where in all cases we have chosen the maximal order of sum rules $k = k_{\max}$ for the computations. The lower bound improves very slowly as l increases (compare [24] for a related result for $d = 1$). In some cases, it is even for $l = 13$ less accurate than the obvious lower bound $s_2(\Phi) - 1 \leq s_\infty(\Phi)$. On the other hand, the upper bound is constant for all $l = 1, \dots, 13$, and gives the exact value, as is theoretically predicted for the first and last examples by the result from [8] which says that L_∞ stability and the additional condition $P(\omega) \geq 0$ implies

$$s_\infty(\Phi) = \bar{s}_\infty^1(\Phi) .$$

Based on the numerical evidence, we anticipate that this holds true also for the second scheme which does not satisfy the non-negative condition for its symbol (although we do not have a strict proof for this claim).

3.2 Approximating rules

We will consider a combination of the rule from Figure 6 a) for updating the dual vertices and a 1-ring update for the old vertices as depicted in Figure 6 b). The symbol for the

l	$\bar{s}_\infty^l(\Phi)$	$\underline{s}_\infty^l(\Phi)$	$\bar{s}_\infty^l(\Phi)$	$\underline{s}_\infty^l(\Phi)$	$\bar{s}_\infty^l(\Phi)$	$\underline{s}_\infty^l(\Phi)$
1	0.7381	-0.2370	1.5401	-0.7734	1.5608	-0.6399
2	0.7381	0.1150	1.5401	-0.4524	1.5608	-0.3478
3	0.7381	0.3293	1.5401	0.1111	1.5608	0.2647
4	0.7381	0.4325	1.5401	0.5216	1.5608	0.6179
5	0.7381	0.4938	1.5401	0.7836	1.5608	0.8047
6	0.7381	0.5346	1.5401	0.8693	1.5608	0.9305
7	0.7381	0.5637	1.5401	0.9948	1.5608	1.0206
8	0.7381	0.5855	1.5401	1.0661	1.5608	1.1407
9	0.7381	0.6024	1.5401	1.1291	1.5608	1.1407
10	0.7381	0.6160	1.5401	1.1705	1.5608	1.1827
11	0.7381	0.6271	1.5401	1.2043	1.5608	1.2170
12	0.7381	0.6364	1.5401	1.2324	1.5608	1.2457
13	0.7381	0.6442	1.5401	1.2562	1.5608	1.2699

Table 2: Upper and lower Hölder smoothness estimates for Table 1 and $l \leq 13$

corresponding scalar refinement relation is given by

$$P(\omega) \hat{=} \frac{1}{3} \begin{bmatrix} 0 & 0 & b & c & b \\ 0 & c & a & a & c \\ b & a & \mathbf{d} & a & b \\ c & a & a & c & 0 \\ b & c & b & 0 & 0 \end{bmatrix}, \quad (40)$$

which is more compact compared to (32).

As before, Condition E and sum rules of order $k \geq 1$ will be satisfied if (33) holds. The calculations of these derivatives is straightforward from (40). For $k = 1$ we have

$$P(\tilde{\omega}^j) = \frac{1}{3}(6c + d) + (a + b)(\tilde{z}^j + \tilde{z}^{2j}),$$

and the conditions are satisfied if

$$3(a + b) = 6c + d = 1. \quad (41)$$

As above, (41) automatically implies sum rules of order $k = 2$. For $k = 3$, we have

$$\begin{aligned} \tilde{D}^{(2,0)}P(\tilde{\omega}^j) &= \tilde{D}^{(0,2)}P(\tilde{\omega}^j) = 4c + \frac{2}{3}(a + 4b)(\tilde{z}^j + \tilde{z}^{2j}), \\ \tilde{D}^{(1,1)}P(\tilde{\omega}^j) &= -2c - \frac{1}{3}(a + 4b)(\tilde{z}^j + \tilde{z}^{2j}), \quad j = 0, 1, 2. \end{aligned}$$

Thus, we have sum rules of order $k = 3$ if the parameters satisfy (41) and

$$a + 4b = 6c. \quad (42)$$

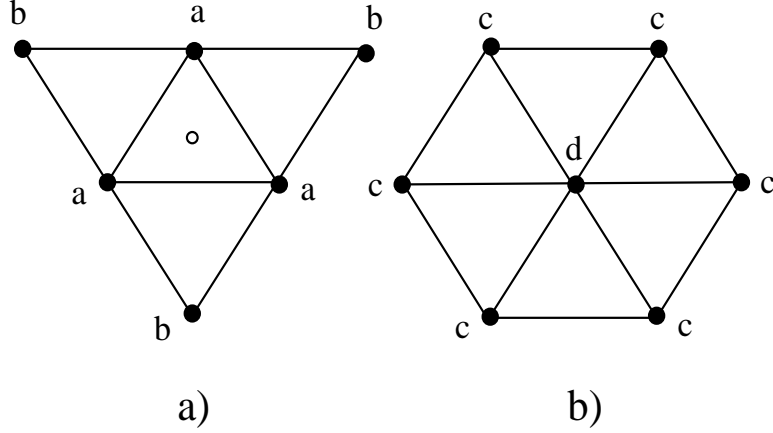


Figure 6: Approximating rule: Stencil for a) dual vertices and b) original vertices

Observing these two conditions still leaves us with a one-parameter family of schemes. Upon setting $b = 0$, we have $a = 1/3$, $c = 1/18$, $d = 2/3$, which is Kobbelt's scheme [16] in the shift-invariant case. It is particularly interesting, since it has a more compact rule for the dual vertices. The other attractive scheme would result from setting $c = 0$, and coincides with the interpolatory rule considered in Section 3.1. Thus, Kobbelt's rule distinguishes itself among all rules with $k = 3$ (we will see in the moment that the sum rule order of this scheme is exactly 3).

Finally, let us check for sum rules of order $k = 4$, where

$$\begin{aligned} \tilde{D}^{(2,1)}P(\tilde{\omega}^j) &= -\tilde{D}^{(1,2)}P(\tilde{\omega}^j) = \frac{1}{3}(a - 8b)(\tilde{z}^j - \tilde{z}^{2j}), \\ \tilde{D}^{(3,0)}P(\tilde{\omega}^j) &= \tilde{D}^{(0,3)}P(\tilde{\omega}^j) = 0, \quad j = 0, 1, 2. \end{aligned}$$

Thus, we obtain one more additional condition,

$$a = 8b, \tag{43}$$

which together with (41) and (42) implies that the only scheme in the considered class with sum rules of order $k = 4$ is given by

$$a = 8/27, \quad b = 1/27, \quad c = 2/27, \quad d = 5/9. \tag{44}$$

Since

$$\tilde{D}^{(4,0)}P(\tilde{\omega}^j) = 12c + \frac{2}{3}(a + 16b)(\tilde{z}^j + \tilde{z}^{2j}) \neq 0,$$

the order $k = 4$ is exact.

The computed values of stability indicators and smoothness exponents for the only scheme with $k_{\max} = 4$, some schemes from the one-parameter family

$$a = \frac{1}{3} - b, \quad c = \frac{1}{18} + \frac{b}{2}, \quad d = \frac{2}{3} - 3b \quad (0 \leq b \leq \frac{2}{9})$$

No.	a	b	c	d	k_{\max}	$\tilde{\nu}_{stab}(\Phi)$	$s_2(\Phi)$	$s_\infty(\Phi)$
1	8/27	1/27	2/27	5/9	4	$0.4951e - 2$	3.9518	3.3143
2	1/3	0	1/18	2/3	3	$0.1850e - 1$	2.9360	2.6309
3	2/9	1/9	1/9	1/3	3	0.0000	≥ 3.0000	≥ 3.0000
4	1/6	1/6	5/36	1/6	3	$0.4340e - 6$	2.9683	2.7491
5	1/9	2/9	1/6	0	3	$0.5461e - 5$	2.4432	2.2849
6	1/3	0	1/9	1/3	2	0.0000	≥ 2.0000	≥ 2.0000
7	1/3	0	1/6	0	2	0.0000	≥ 1.9172	≥ 1.4321

Table 3: Sobolev and Hölder smoothness for some schemes with symbol (40)

with $k_{\max} = 3$, and two more schemes with $k_{\max} = 2$ are shown in Table 3. The stability indicators $\tilde{\nu}_{stab}$ correctly predict the schemes with unstable Φ (although the numbers in the 4th and 5th row of Table 3 are relatively small, the internally set error tolerances in the used routine are such that values $\tilde{\nu}_{stab} \geq 1e - 8$ safely indicate L_2 -stability). Figure 7 shows the graphs of some of the associated refinable functions.

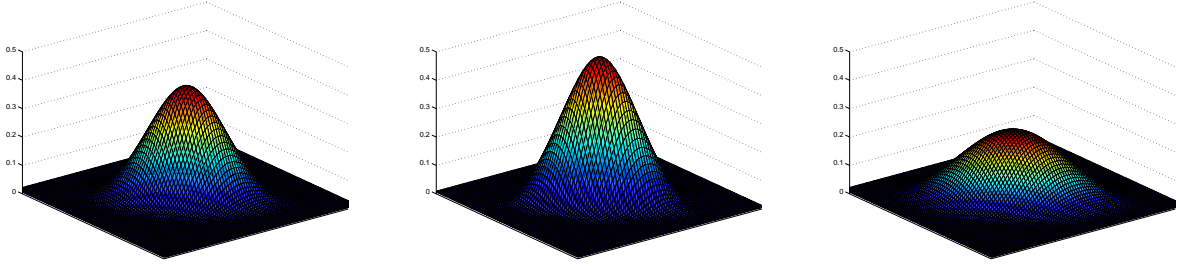


Figure 7: Basis functions for the approximating schemes No. 1-3 of Table 3

The scheme (44) stands out as the one with stable Φ , where the order of sum rules is maximal: both Sobolev and Hölder smoothness exceed 3 in this case. The other remarkable choice is

$$a = 2/9, \quad b = 1/9, \quad c = 1/9, \quad d = 1/3, \quad (45)$$

where we recover the lowest order box spline construction related to $\sqrt{3}$ -subdivision. The refinable function is a C^3 quartic box spline [2] associated with the direction set

$$\Theta = \begin{bmatrix} 1 & 0 & -1 & 1 & -2 & 1 \\ 0 & -1 & 1 & -2 & 1 & 1 \end{bmatrix}.$$

Its integer shifts feature linear dependencies, and the order of sum rules is smaller than the polynomial accuracy. Our methods for computing the Hölder continuity fail since the assumption (29) in Theorem 5 cannot be satisfied. The critical Sobolev and Hölder exponents are obviously $s_2(\Phi) = 4.5$ and $s_\infty(\Phi) = 4$ in this case. This is because the

limiting surface is piecewise quartic C^3 with respect to a Powell-Sabin split of the initial triangulation. The examples with $k_{\max} = 2$ in Table 3 have unstable Φ (concerning scheme No. 6, see the discussion at the end of Section 3.3).

It should be noted that most of the Hölder exponents shown in the last column of Table 3 are *anticipated* values based on the numerical evidence reported in Table 4. The exception is the first scheme, where one can prove $P(\omega) \geq 0$ and, thus, rely on the above-mentioned characterization of the critical Hölder exponent from [8]. While the lower bounds always monotonously but slowly increase, the upper bounds remain constant in Examples 1-3 and 6-7. In the remaining two examples this is not the case, and the computed upper bounds suggest that now $\bar{\alpha}_{\infty}^2(\Phi)$ (and not $\bar{\alpha}_{\infty}^1(\Phi)$) represents the correct value of the critical Hölder exponent. This is the value we have subsequently taken for the last column of Table 3.

3.3 Dual schemes

We discuss now the smoothness issue for some of the *composite primal/dual $\sqrt{3}$ -subdivision schemes* introduced in [21]. Such schemes are obtained through composition of some elementary geometric rules involving the z -values associated with the same or different types of topologic elements (i.e., vertices (V), edges (E), and triangles or faces (F)), and a very simple primal subdivision step. Examples of such rules are given in Figure 8. The parameters will always be chosen such that at least constants are reproduced (e.g., we must have $c = 1/6$ for the FV and EV rules, $d = 1/3$ for the EF rule, and $e = 1/2$ for the FE rule). E.g., applying the FV -rule on the original grid, followed by

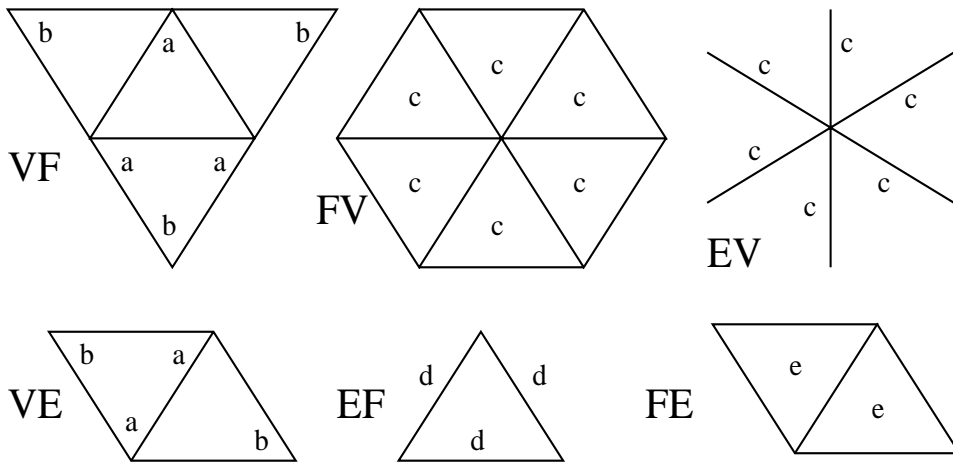


Figure 8: Some elementary rules

an interpolatory subdivision step using (1), and the application of the VF -rule on the refined grid results in a composite F -based or dual $\sqrt{3}$ -subdivision scheme. Note that F -based schemes lead to vector refinement equations with $r = 2$.

	Example 1		Example 2		Example 3		Example 4	
l	$\overline{s}_\infty^l(\Phi)$	$\underline{s}_\infty^l(\Phi)$	$\overline{s}_\infty^l(\Phi)$	$\underline{s}_\infty^l(\Phi)$	$\overline{s}_\infty^l(\Phi)$	$\underline{s}_\infty^l(\Phi)$	$\overline{s}_\infty^l(\Phi)$	$\underline{s}_\infty^l(\Phi)$
1	3.3142	0.6658	2.6309	0.2584	3.0000	0.7780	3.0000	1.2244
2	3.3142	1.2107	2.6309	0.7154	3.0000	1.3311	2.7491	1.6549
3	3.3142	1.8107	2.6309	1.1944	3.0000	1.7356	2.9550	1.8659
4	3.3142	2.1759	2.6309	1.5319	3.0000	1.9665	2.7491	2.0358
5	3.3142	2.3990	2.6309	1.7384	3.0000	2.1661	2.9419	2.1555
6	3.3142	2.5522	2.6309	1.8946	3.0000	2.2756	2.7491	2.2280
7	3.3142	2.6608	2.6309	1.9825	3.0000	2.3858	2.9092	2.2938
8	3.3142	2.7427	2.6309	2.0766	3.0000	2.4484	2.7491	2.3416
9	3.3142	2.8061	2.6309	2.1209	3.0000	2.5176	2.8884	2.3841
10	3.3142	2.8570	2.6309	2.1855	3.0000	2.5566	2.7491	2.4200
11	3.3142	2.8985	2.6309	2.2105	3.0000	2.6040	2.8766	2.4484

	Example 5		Example 6		Example 7	
l	$\overline{s}_\infty^l(\Phi)$	$\underline{s}_\infty^l(\Phi)$	$\overline{s}_\infty^l(\Phi)$	$\underline{s}_\infty^l(\Phi)$	$\overline{s}_\infty^l(\Phi)$	$\underline{s}_\infty^l(\Phi)$
1	2.4531	0.7431	2.0000	0.0851	1.4321	0.2247
2	2.2849	1.3167	2.0000	0.5278	1.4321	0.6872
3	2.4423	1.5664	2.0000	0.8207	1.4321	0.9557
4	2.2849	1.7048	2.0000	1.0207	1.4321	1.1157
5	2.3568	1.8089	2.0000	1.1654	1.4321	1.1997
6	2.2849	1.8831	2.0000	1.2750	1.4321	1.2499
7	2.3438	1.9476	2.0000	1.3605	1.4321	1.2774
8	2.2849	1.9762	2.0000	1.4289	1.4321	1.3018
9	2.3231	2.0210	2.0000	1.4848	1.4321	1.3170
10	2.2849	2.0401	2.0000	1.5313	1.4321	1.3309
11	2.3226	2.0728	2.0000	1.5704	1.4321	1.3406

Table 4: Upper and lower Hölder smoothness estimates for Table 3 and $l \leq 11$

The symbol of a vector refinement equation resulting from composite schemes possesses factorizations in terms of the symbols of the elementary steps. For instance, in the above example of an F -based composite rule, with the VF -rule from Figure 8 specified by $a = 1/3$, $b = 0$, we would have

$$P^{FF}(\omega) = P^{FV}(M^T\omega)P^{VV}(\omega)P^{VF}(\omega) = P^{VV}(\omega)(P^{FV}(M^T\omega)P^{VF}(\omega)), \quad (46)$$

where the scalar symbol $P^{VV}(\omega)$ coincides with (32) for $a = 1/3$, $b = c = 0$, while the 2×1 and 1×2 symbol matrices

$$P^{FV}(\omega) \triangleq \frac{1}{3} \begin{pmatrix} \begin{bmatrix} 0 & 0 & 0 \\ 0 & \mathbf{1} & 1 \\ 0 & 1 & 0 \end{bmatrix} \\ \begin{bmatrix} 0 & 0 & 0 \\ 0 & \mathbf{0} & 1 \\ 0 & 1 & 1 \end{bmatrix} \end{pmatrix}, \quad P^{VF}(\omega) \triangleq \frac{1}{6} \left(\begin{bmatrix} 0 & 1 & 0 \\ 1 & \mathbf{1} & 0 \\ 0 & 0 & 0 \end{bmatrix} \begin{bmatrix} 1 & 1 & 0 \\ 1 & \mathbf{0} & 0 \\ 0 & 0 & 0 \end{bmatrix} \right),$$

correspond to the FV -rule on the coarse triangulation, and the simpler VF -rule on the $\sqrt{3}$ -refined triangulation, respectively. Our matrix notation is always such that the two functions ϕ_1^{FF} and ϕ_2^{FF} which compose the refinable vector Φ^{FF} associated with the mask P^{FF} of a F -based scheme correspond to the triangles with vertices $(0, 0)$, $(1, 0)$, $(0, 1)$ and $(1, 0)$, $(0, 1)$, $(1, 1)$, respectively, while the scalar refinable function $\phi^{VV} = \Phi^{VV}$ of the V -based scheme is attached to the origin. Note that the matrix symbol (46) has rank 1, and could therefore be considered as essentially scalar. It is easy to guess that many of the properties of this composite F -based scheme are similar to those of a V -based subdivision scheme with symbol

$$\tilde{P}^{VV}(\omega) := P^{VV}(\omega)(P^{VF}(\omega)P^{FV}(\omega)), \quad (47)$$

represented by the product of two scalar trigonometric functions.

Such factorizations are very handy. Sum rules can be checked by examination of the factors. E.g., if $P^{VV}(\omega)$ has sum rules of order k_1 and $P^{FV}(M^T\omega)P^{VF}(\omega)$ sum rules of order k_2 then $P^{FF}(\omega)$ has sum rules of order $k_1 + k_2$. This immediately follows from the definition (16), the Leibniz rule for differentiation of products, and the fact that the symbol $P^{VV}(\omega)$ is scalar. Moreover, factorizations can be used to simplify the smoothness computations (however, we do not make use of the last observation).

Let us give some details for the scheme with symbol (46). Observe that the scalar symbol

$$P^{VV,1}(\omega) := P^{VF}(\omega)P^{FV}(\omega) \triangleq \frac{1}{9} \begin{bmatrix} 0 & 1 & 1 \\ 1 & \mathbf{3} & 1 \\ 1 & 1 & 0 \end{bmatrix}$$

which appears in the factorization (47) coincides with the one for the interpolatory method (1). Thus, the properties of a vector refinement equation with symbol

$$P^{FF,1}(\omega) := P^{FV}(M^T\omega)P^{VF}(\omega),$$

should be closely related to it. Since the maximal order of sum rules for $P^{VV,1}(\omega)$ is $k_{\max} = 2$, we have $k \leq 2$ for $P^{FF,1}(\omega)$. Using the factorization we can write the conditions for sum rules of order $k = 1$ as follows: There exists a 1×2 vector of trigonometric polynomials $B(\omega)$ such that

$$\tilde{B}(0)P^{VF}(\tilde{\omega}^j) = \delta(j)B(0), \quad j = 0, 1, 2, \quad \tilde{B}(\omega) := B(\omega)P^{FV}(\omega).$$

Since $P^{VF}(\tilde{\omega}^j) = \delta(j)(1/2, 1/2)$ and $P^{FV}(0) = (1, 1)^T$, we conclude that $k = 1$ holds: just choose $B(\omega)$ such that $B(0) = (1, 1)$.

However, sum rules of order $k = 2$ cannot hold since they would require

$$\sigma(D_{\Lambda}^{\nu}\tilde{B})(0)P^{VF}(\tilde{\omega}^j) + \tilde{B}(0)(D_{\Lambda}^{\nu}P^{VF})(\tilde{\omega}^j) = \delta(j)(D_{\Lambda}^{\nu}B)(0)$$

for both $\nu = (1, 0)$ and $\nu = (0, 1)$. For $j = 1, 2$ this implies $(D_{\Lambda}^{\nu}P^{VF})(\tilde{\omega}^j) = (0, 0)$ or, equivalently,

$$(\tilde{D}^{\nu}P^{VF})(\tilde{\omega}^j) = (0, 0), \quad j = 1, 2, \quad |\nu| = 1.$$

Now, a direct computation of these derivatives from the above formula yields

$$(D^{(1,0)}P^{VF})(\tilde{\omega}^j) = -\frac{1}{6}(\tilde{z}^{2j}, 1 + \tilde{z}^{2j}) \neq (0, 0),$$

which is the desired contradiction. On the other hand, from [21] we have the formula

$$\hat{\Phi}^{FF,1}(\omega) = P^{FV}(\omega)\hat{\phi}^{VV,1}(\omega) \tag{48}$$

for the Fourier transforms for the refinable 2×1 function $\Phi^{FF,1}(x)$ resp. the refinable function $\phi^{VV,1}(x)$ (i.e., the solutions of refinement equations with symbols $P^{FF,1}(\omega)$ resp. $P^{VV,1}(\omega)$) satisfying $\hat{\Phi}^{FF,1}(0) = (1, 1)^T$ resp. $\hat{\phi}^{VV,1}(0) = 1$. As a consequence,

$$\begin{aligned} \phi_1^{FF,1}(x) &= \frac{1}{3}(\phi^{VV,1}(x) + \phi^{VV,1}(x - e^1) + \phi^{VV,1}(x - e^2)), \\ \phi_2^{FF,1}(x) &= \frac{1}{3}(\phi^{VV,1}(x - e^1) + \phi^{VV,1}(x - e^2) + \phi^{VV,1}(x - e^1 - e^2)), \end{aligned}$$

where e^1, e^2 are the unit vectors in \mathbb{Z}^2 . In particular, the refinable vector-valued functions related to the symbol $P^{FF,1}(\omega)$ are as smooth as the refinable functions related to the symbol $P^{VV,1}(\omega)$. On the other hand, there are local linear dependencies in the set $\Phi^{FF,1}$ of integer shifts of $\phi_1^{FF,1}, \phi_2^{FF,1}$ as we obviously have

$$\begin{aligned} \phi_1^{FF,1}(x) + \phi_1^{FF,1}(x + e^1) + \phi_1^{FF,1}(x + e^2) \\ = \phi_2^{FF,1}(x + e^1) + \phi_2^{FF,1}(x + e^2) + \phi_2^{FF,1}(x + e^1 + e^2). \end{aligned}$$

In terms of subdivision this means that if we start with an oscillating ± 1 pattern of z_{Δ} -values around a regular vertex then, after one subdivision step, this oscillation has disappeared. In other words, the above linear dependencies correspond to 0-eigenvalues of the subdivision operator, and are harmless.

Before we go on, let us comment on the choice of the V -based subdivision scheme with symbol $P^{VV}(\omega)$ in the overall composite scheme. We can choose any of the schemes of Section 3.1 and 3.2, or even set $P^{VV}(\omega) = 1$. The above findings will not change, except that everywhere symbols $P^{VV,1}(\omega)$ have to be replaced by $\tilde{P}^{VV}(\omega) = P^{VV}(\omega) \cdot P^{VV,1}(\omega)$. The refinable functions will be convolutions of $\phi^{VV}(x)$ and $\phi^{VV,1}(x)$, i.e., much smoother. A particularly simple and natural choice is to set

$$P^{VV,n}(\omega) = \underbrace{P^{VV,1}(\omega) \cdot \dots \cdot P^{VV,1}(\omega)}_{n \text{ times}} = P^{VV,1}(\omega)^n \quad (49)$$

and

$$P^{FF,n}(\omega) = P^{VV,n-1}(\omega)P^{FF,1}(\omega) = P^{VV,1}(\omega)^{n-1}P^{FF,1}(\omega). \quad (50)$$

The symbol (49) corresponds to a primal $\sqrt{3}$ -subdivision scheme which we call (VV, n) -scheme. It can be performed as a trivial primal upsampling operation with symbol $P(\omega) = 1$ (which assigns zeros to the new vertices, and $3z_V$ to the old vertices of the refined triangulation) followed by n times alternatively applying the simple VF - and FV -rules given above on the refined triangulation. Similarly, the symbol (50) leads to the dual (FF, n) -scheme which can be performed by applying the FV -rule on the coarse grid, followed by the primal $(VV, n-1)$ -scheme as described above and a final VF -rule on the refined triangulation. Note that the (FF, n) -scheme has sum rules of order $2n-1$ while the (VV, n) -scheme has sum rules of order $2n$. The smoothness of the schemes is, however, the same and governed by the properties of $P^{VV,n}(\omega)$. It is interesting to mention that $P^{VV,2}(\omega)$ coincides with the symbol (40) corresponding to the family of approximating schemes studied in Section 3.2 for the parameter choice (44). Thus, the $(FF, 2)$ -scheme which can be performed as a sequence of one FV -step on the coarse triangulation, a subdivision step using (1), and a VF -step on the refined triangulation, already leads to C^3 -surfaces and looks quite attractive.

Unfortunately, there is no trivial choice of VF -rule, V -based subdivision scheme, and FV -rule such that $\tilde{P}^{VV}(\omega)$ (the symbol (47) related to the V -based counterpart of the resulting composite F -based scheme) turns into the symbol (40) for the parameter choice (45). However, there is a choice of *generalized VF - and FV -rules*, complemented by trivial upsampling (i.e., $P^{VV}(\omega) = 1$) as subdivision step, which yields (40) with the parameters (45) and thus leads to C^3 quartic box spline surfaces for the F -based scheme, too. The rules are shown (for the shift-invariant case) in Figure 9. As above, the resulting refinable vector-valued function $\Phi^{FF}(x)$ can be expressed componentwise by linear combinations of the C^3 quartic box splines $\phi^{VV}(x)$ associated with the V -based scheme (40), (45). E.g.,

$$\begin{aligned} \phi_1^{FF}(x) &= \frac{2}{9}(\phi^{VV}(x) + \phi^{VV}(x - e^1) + \phi^{VV}(x - e^2)) \\ &\quad + \frac{1}{9}(\phi^{VV}(x - e^1 - e^2) + \phi^{VV}(x - e^1 + e^2) + \phi^{VV}(x + e^1 - e^2)), \end{aligned}$$

analogously for $\phi_2^{FF}(x)$.

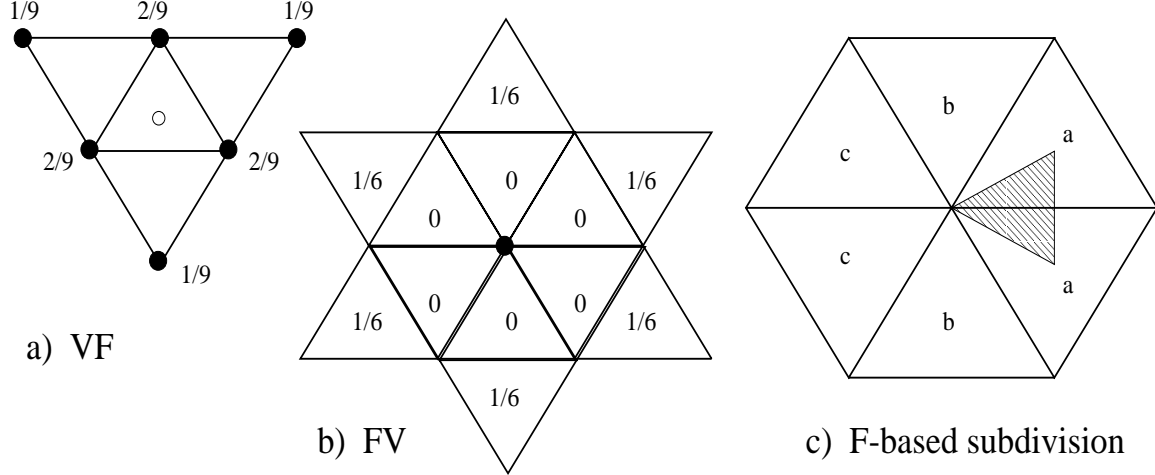


Figure 9: Generalized FV - and VF -rules and ad hoc F -based scheme

n	$k_{\max}^{VV,n}$	$k_{\max}^{FF,n}$	$\nu_{stab}(\Phi^{VV,n})$	$\tilde{\nu}_{stab}(\Phi^{VV,n})$	$s_2(\Phi^{VV,n})$	$s_{\infty}(\Phi^{VV,n})$
1	2	1	0.1262	0.1262	1.6571	0.7381
2	4	3	$0.4951e - 2$	$0.4951e - 2$	3.9518	3.3143
3	6	5	$0.2009e - 3$	$0.2009e - 3$	5.9960	5.7073
4	8	7	$0.8159e - 5$	$0.8159e - 5$	7.9997	7.9036

Table 5: Sobolev and Hölder smoothness for (VV, n) -schemes

In Table 5 we report the numerical results for the (VV, n) - and (FF, n) -schemes with $n \leq 4$. As explained above, the cases $n = 1$ and $n = 2$ have already appeared in Table 1 and 3, respectively. For values $n \geq 5$, due to the high order of sum rules and larger dimensions of the computational invariant subspace for T_P (for $n = 5$ we already have dimension 293, after restricting to symmetric matrices), numerical instabilities reduce the reliability of the computed values. Note that the computed Hölder exponents are exact, since $P^{VV,n}(\omega) = P^{VV,1}(\omega)^n \geq 0$. Since the (FF, n) -schemes inherit their smoothness properties from the (VV, n) -schemes, there is no need to perform additional computations for them.

We finish with the investigation for an *ad hoc* choice of a simple three-parameter family of dual $\sqrt{3}$ -subdivision schemes which are not based on composite rules. The parameters of these rules are shown in Figure 9 c): the z -value for the shaded face in the $\sqrt{3}$ -refined triangulation is defined as a weighted average of the z -values of old faces around the common vertex in the unrefined mesh. After an appropriate index shift, the

associated symbol takes the following form:

$$P(\omega) \doteq \frac{1}{3} \begin{pmatrix} \begin{bmatrix} 0 & 0 & 0 & 0 & c \\ 0 & 0 & b & a & b \\ 0 & c & \mathbf{a} & a & 0 \\ 0 & 0 & b & c & 0 \\ 0 & 0 & 0 & 0 & 0 \end{bmatrix} & \begin{bmatrix} 0 & 0 & 0 & b & c \\ 0 & c & a & a & 0 \\ 0 & b & \mathbf{a} & b & 0 \\ 0 & 0 & c & 0 & 0 \\ 0 & 0 & 0 & 0 & 0 \end{bmatrix} \\ \begin{bmatrix} 0 & 0 & 0 & 0 & 0 \\ 0 & 0 & c & 0 & 0 \\ 0 & b & \mathbf{a} & b & 0 \\ 0 & a & a & c & 0 \\ c & b & 0 & 0 & 0 \end{bmatrix} & \begin{bmatrix} 0 & 0 & 0 & 0 & 0 \\ 0 & c & b & 0 & 0 \\ 0 & a & \mathbf{a} & c & 0 \\ b & a & b & 0 & 0 \\ c & 0 & 0 & 0 & 0 \end{bmatrix} \end{pmatrix}. \quad (51)$$

Even before starting any investigation, it is clear that the resulting 2×1 refinable vector $\Phi = (\phi_1, \phi_2)^T$ is unstable, independently of the parameter choices. Indeed, using the refinement relations one can easily check that

$$\sum_{\alpha \in \mathbb{Z}^2} (1, -1) \cdot \Phi(x - \alpha) = 0, \quad x \in \mathbb{R}^2,$$

which implies the linear dependence of the set Φ of shifts, and the L_p -instability of Φ if $\Phi \in L_p(\mathbb{R}^2)^{2 \times 1}$.

We start with the investigation of sum rules. For $k = 1$, (20) is equivalent to $b^{(0,0)}P(\tilde{\omega}^j) = \delta(j)b^{(0,0)}$, for $j = 0, 1, 2$, with $b^{(0,0)} \neq 0$. I.e., as already expressed by the notation, $b^{(0,0)}$ is a left 1-vector of $P(0)$, i.e., a multiple of b^0 . We compute

$$P(\tilde{\omega}^j) = \frac{a+b+c}{3} p(\tilde{z}^j) \begin{pmatrix} 1 & 1 \\ 1 & 1 \end{pmatrix} = \delta(j)(a+b+c) \begin{pmatrix} 1 & 1 \\ 1 & 1 \end{pmatrix}, \quad j = 0, 1, 2, \quad (52)$$

since $p(z) \equiv 1 + z + z^2$ vanishes for $z = \tilde{z}^j$, $j = 1, 2$. Thus, the condition

$$a + b + c = \frac{1}{2} \quad (53)$$

is necessary (and sufficient) for sum rules of order 1, Condition E for $P(0)$ is automatically satisfied (the second eigenvalue of $P(0)$ is 0). Without loss of generality, we set $b^{(0,0)} = (1, 1)$.

To find out whether sum rules of order $k = 2$ are feasible, we make the following simplifying observation. If we put $\mu = (1, 0)$ or $\mu = (0, 1)$ then the expression on the left-hand side of (20) contains exactly two terms. According to (52), $P(\tilde{\omega}^j)$ is a zero matrix for $j = 1, 2$ which gives

$$b^{(0,0)}(D_1 - \tilde{z}D_2)P(\tilde{\omega}^j) = b^{(0,0)}(D_1 - \tilde{z}^2D_2)P(\tilde{\omega}^j) = (0, 0), \quad j = 1, 2,$$

or, equivalently,

$$\tilde{D}^{(1,0)}(b^{(0,0)}P)(\tilde{\omega}^j) = \tilde{D}^{(0,1)}(b^{(0,0)}P)(\tilde{\omega}^j) = (0, 0), \quad j = 1, 2.$$

a	b	c	k_{\max}	$s_2(\Phi)$	$s_\infty(\Phi)$
1/3	1/6	0	2	1.9388	1.4321
17/48	1/8	1/48	2	1.9730	1.5702
13/36	1/9	1/36	2	1.9821	1.6334
9/24	1/12	1/24	2	1.9952	1.7927
7/18	1/18	1/18	3	2.6723	2.1239
6/15	1/30	1/15	2	1.9951	1.6681
5/12	0	1/12	2	1.8661	1.2619

Table 6: Numerical results for F -based schemes given by (51), (56)

Since

$$b^{(0,0)}P(\omega) \doteq \frac{1}{3} \left(\begin{array}{ccccc} \left[\begin{array}{ccccc} 0 & 0 & 0 & 0 & c \\ 0 & 0 & b+c & a & b \\ 0 & b+c & \mathbf{2a} & a+b & 0 \\ 0 & a & a+b & 2c & 0 \\ c & b & 0 & 0 & 0 \end{array} \right] & \left[\begin{array}{ccccc} 0 & 0 & 0 & b & c \\ 0 & 2c & a+b & a & 0 \\ 0 & b+a & \mathbf{2a} & b+c & 0 \\ b & a & b+c & 0 & 0 \\ c & 0 & 0 & 0 & 0 \end{array} \right] \end{array} \right),$$

we easily compute that the above derivative values vanish if and only if

$$a = 2b + 5c. \quad (54)$$

Moreover,

$$b^{(1,0)} = -\frac{1-\tilde{z}}{6}(1, -1), \quad b^{(0,1)} = -\frac{1-\tilde{z}^2}{6}(1, -1), \quad (55)$$

which follows by examining (20) for $j = 0$.

For the case $k = 3$, computations become very tedious, and we state only the result (see the extended version of this paper for full details). We found that in the one-parameter family of rules given by

$$a = \frac{1}{3} + c, \quad b = \frac{1}{6} - 2c, \quad c \in \mathbb{R}, \quad (56)$$

for which $k \geq 2$ has been established (compare (53) and (54)), only the case $c = 1/18$ leads to $k_{\max} = 3$.

In Table 6, we report some representative results for the parameter family (56). We restricted our attention to schemes with non-negative coefficients $a, b, c \geq 0$. As expected, the stability indicators vanished, and we do not show them. The shown values in the last two columns of Table 6 are only (anticipated) lower bounds for the smoothness exponents, even though we believe that they represent the exact values.

Let us finish with the following observations. The previously discussed composite $(FF, 1)$ -rule which is related to the primal interpolatory rule (1) possesses a symbol of the form (51) with $a = b = c = 1/6$. Thus, for these parameters our ad hoc F -based scheme has only $k_{\max} = 1$, although the Sobolev smoothness of this refinable vector Φ

is well above 1 according to the result for the scalar case. Theoretically, there might be other composite schemes among those with symbol (51) which would open another avenue to investigate them. In particular, one might ask whether the exceptional scheme with $k_{\max} = 3$, i.e.,

$$a = \frac{7}{18}, \quad b = c = \frac{1}{18}, \quad (57)$$

is associated with a composite rule. The answer is yes, although we need to extend our view of composite rules a bit. The composite scheme starts with face values on the coarse triangulation and computes vertex values on the refined triangulation: values at old vertices are obtained by averaging (see the FV -rule in Figure 8) while the value at a face is assigned directly to the associated new dual vertex, i.e., to its barycenter. After this, face values on the finer triangulation are computed by the averaging VF -rule from Figure 8. It is not hard to verify that the resulting F -based subdivision scheme has the symbol (51) with the parameters (57). As above, we can now find the associated V -based scheme. It turns out (we leave this as an exercise for the interested reader) that we arrive at an approximate scheme of the type discussed in Section 3.2, with parameters

$$a = d = 1/3, \quad b = 0, \quad c = 1/9. \quad (58)$$

Unfortunately, the scalar Φ for this set of parameters is also unstable (see Table 3), and the maximal order of sum rules is only $k_{\max} = 2$, i.e., below the one in the vector case. Thus, we do not benefit for the theoretical analysis of the F -based scheme here (rather, we could use the smoothness bounds obtained for the F -based scheme (57) to improve the smoothness bounds for the corresponding V -based scheme with parameters (58) in Table 3).

References

- [1] A. Barinka, S. Dahlke, N. Mulders, The IGPM Vилlemoes machine, IGPM-Report 184, RWTH Aachen, February 2000.
- [2] C. de Boor, K. Höllig, S. D. Riemenschneider, Box Splines, Appl. Math. Sciences vol. 98, Springer, New York, 1993.
- [3] A. S. Cavaretta, W. Dahmen, C. A. Micchelli, Stationary subdivision, Memoirs AMS, vol. 93, AMS, Providence, 1991.
- [4] A. Cohen, K. Gröchenig, L. F. Vилlemoes, Regularity of multivariate refinable functions, Constr. Approx. 15 (1999) 241–255.
- [5] S. Dahlke, K. Gröchenig, P. Maass, A new approach to interpolating scaling functions, Appl. Anal. 72 (3-4) (1999) 485–500.
- [6] S. Dahlke, P. Maass, G. Teschke, Interpolating scaling functions with duals, J. Comput. Anal. Appl. 5 (3) (2003) 361–373.

- [7] T. Eirola, Sobolev characterization of solutions of dilation equations, *SIAM J. Math. Anal.* 23 (1992), 1015–1030.
- [8] H. Ji, S. D. Riemenschneider, Z. Shen, Multivariate compactly supported fundamental refinable functions, duals, and biorthogonal wavelets, *Stud. Appl. Math.* 102 (1999), 173–204.
- [9] R. Q. Jia, Characterization of smoothness of multivariate refinable functions in Sobolev spaces, *Trans. Amer. Math. Soc.* 351 (1999), 4089–4112.
- [10] R. Q. Jia, Q. Jiang, Characterization of smoothness of multivariate refinable vectors, Manuscript, 2000.
- [11] R. Q. Jia, K. S. Lau, D. X. Zhou, L_p -solutions of refinement equations, *J. Fourier Anal. Appl.* 7 (2001), 143–167.
- [12] R. Q. Jia, C. A. Micchelli, On linear independence of integer translates of a finite number of functions, *Proc. Edinburgh Math. Soc.* 36 (1992), 69–85.
- [13] R. Q. Jia, S. D. Riemenschneider, D. X. Zhou, Vector subdivision schemes and multiple wavelets, *Math. Comp.* 67 (1998), 1533–1563.
- [14] R. Q. Jia, S. R. Zhang, Spectral properties of the transition operator associated to a multivariate refinement equation, *Linear Algebra Appl.* 292 (1999), 155–178.
- [15] Q. T. Jiang, Multivariate matrix refinable functions with arbitrary matrix dilation, *Trans. Amer. Math. Soc.* 351 (1999), 2407–2438.
- [16] L. Kobbelt, $\sqrt{3}$ -subdivision, in *Proceedings SIGGRAPH 2000 (July 2000)* 103–112.
- [17] U. Labsik, G. Greiner, Interpolatory $\sqrt{3}$ -subdivision, *Computer Graphics Forum*, 19 (3) (2000) 131–138.
- [18] R. Lorentz, P. Oswald, Criteria for hierarchical bases in Sobolev spaces, *Appl. Comput. Harmon. Anal.* 8 (2000), 32–85.
- [19] C. A. Micchelli, T. Sauer, On vector subdivision, *Math. Z.* 229 (1998), 621–674.
- [20] P. Oswald, On norm bounds for iterated intergrid transfer operators, *Arbeitsberichte der GMD 1079*, GMD, St. Augustin, June 1997.
- [21] P. Oswald, P. Schröder, Composite primal/dual $\sqrt{3}$ -subdivision schemes, *Comput. Aided Geom. Design*, to be published.
- [22] H. Prautzsch, W. Boehm, Box splines, in “*The Handbook of Computer Aided Geometric Design*”, G. Farin, J. Hoschek, M.-S. Kim (eds.), Elsevier, Amsterdam, 2002, pp. 255–282.

- [23] U. Reif, A unified approach to subdivision algorithms near extraordinary points, *Comput. Aided Geom. Design* 12 (1995), 153–174.
- [24] O. Rioul, Simple regularity criteria for subdivision schemes, *SIAM J. Math. Anal.* 23 (1992), 1544–1576.
- [25] A. Ron, Z. Shen, The Sobolev regularity of refinable functions, *J. Approx. Th.* 106 (2000), 185–225.
- [26] A. Ron, Z. Shen, K. C. Toh, Computing the Sobolev regularity of refinable functions by the Arnoldi method, *SIAM J. Matrix Anal. Appl.* 23 (2001), 57–76.
- [27] Z. Shen, Refinable function vectors, *SIAM J. Math. Anal.* 29 (1998), 235–250.
- [28] G. Umlauf, Analyzing the characteristic map of triangular subdivision schemes. *Constr. Approx.* 16 (2000), 145–155.
- [29] L. Villedieu, Energy moments in time and frequency for two-scale difference equation solutions and wavelets, *SIAM J. Math. Anal.* 23(1992), 1519–1543.
- [30] L. Villedieu, Wavelet analysis of refinement equations, *SIAM J. Math. Anal.* 25 (1994), 1433–1460.
- [31] T. Yu, Parametric families of Hermite subdivision schemes in dimension 1, Preprint, RPI, 1999.
- [32] D. Zorin, Smoothness of stationary subdivision on irregular meshes, *Constr. Approx.* 16 (2000), 359–397.